We are IntechOpen, the world's leading publisher of Open Access books Built by scientists, for scientists

4,800
Open access books available

122,000
International authors and editors

135M
Downloads

Our authors are among the

154
Countries delivered to

TOP 1%
most cited scientists

12.2%
Contributors from top 500 universities

CLARIVATE ANALYTICS BOOK CITATION INDEX INDEXED

WEB OF SCIENCE™

Selection of our books indexed in the Book Citation Index in Web of Science™ Core Collection (BKCI)

Interested in publishing with us?
Contact book.department@intechopen.com

Numbers displayed above are based on latest data collected.
For more information visit www.intechopen.com

6

Clarification of Adsorption Reversibility on Granite that Depends on Cesium Concentration

Keita Okuyama and Kenji Noshita
Hitachi Research Laboratory, Hitachi, Ltd.
Japan

1. Introduction

Disposal of high-level radioactive wastes (HLW) is planned to be done in a repository located deep underground to isolate radionuclides from the biosphere. In case of a leakage accident of HLW, there will be no hazardous impact to humans because migration of the leaked radionuclides will be retarded by matrix diffusion and adsorption on the rock surface. Therefore, the geochemical retardation behavior of radionuclides in aquifers must be clarified, from the viewpoint of the performance assessment of HLW deep underground disposal.

Radionuclide-adsorbed sites in rock are classified into two general types: reversible adsorption sites, where desorption of once-adsorbed nuclides occurs (e.g., an ion-exchange reaction); and irreversible adsorption sites, where only adsorption occurs (e.g., a mineralization reaction). In the early stage of radionuclide leakage, migration of the radionuclides will be retarded by both reversible and irreversible adsorption sites. However, when the irreversible sites are filled, the radionuclides will no longer be retarded by them. Therefore, it is necessary to investigate the sorption reversibility to clarify the behavior of radionuclides (Fukui, 2004).

Cesium-137 (^{137}Cs), which is one of the principal radioactive sources of HLW for 1000 years after geological disposal, is partially fixed in the interlayer of micas and it might be trapped irreversibly in these sites (Francis & Brinkley, 1976). Another report suggested that Cs adsorption on granite has a nonlinear relationship with its concentration in solution (Ohe, 1984). These findings imply it is possible to characterize Cs adsorption on granite. One of the important characterization factors is the adsorption amount on reversible and irreversible sites, which may change with Cs concentration; however, it has not been reported.

The purpose of this study is to clarify Cs adsorption reversibility on granite that depends on Cs concentration by adsorption and sequential extraction experiments, using a variety of chemical reagents for various inlet Cs concentrations (1.0×10^{-3} - 1.0×10^{0} mol/m^3). For the experiments, a narrow flow channel was formed on a granite specimen (Okuyama, et al., 2008). Breakthrough curves (BTCs) were obtained by injecting a Cs solution labeled with

^{134}Cs into the channel. We estimated the amounts diffused into the rock matrix and absorbed on the rock surface. In order to verify the estimated sorption amount, we obtained the retardation coefficient by analyzing BTCs, and compared the value with that calculated using the distribution coefficient (*Kd*) obtained by a batch sorption experiment. After injecting ^{134}Cs solution, extraction reagents (HCl, $CaCl_2$, and KCl solutions) were injected into the flow channel in sequence. We obtained the desorption curves and investigated the chemical speciation of Cs in granite. In particular, we focused on the dependence of adsorption amount on reversible and irreversible sites on Cs concentration.

2. Experiment

2.1 Materials

Biotite granite from the Makabe area of Japan was used in this work. The chemical composition was measured by fluorescent X-ray analysis and the results are listed in Table 1. The mineral composition was also graphically determined using a polarization microscope and these results are listed in Table 2. The porosity of a granite specimen was measured by the water saturation method (Skagius & Neretnieks, 1986), and 0.73 % was obtained. The cation-exchange capacity was determined by the Peech method (Peech, 1965), and 5.9 meq/100g was obtained.

2.2 Adsorption and sequential extraction experiments

In order to clarify sorption reversibility of Cs on granite, we carried out adsorption and sequential extraction experiments. All specimens were cut as a parallelepiped with dimensions of 20 mm × 4 mm × 3 mm and their surfaces were polished with abrasive paper (#1200). The side edge surfaces were thickly coated with an epoxy resin to avoid evaporation of the test solution during experiments (Fig.1). A container was filled with distilled water (pH adjusted to 6 using HCl and NaOH) and set in a glass bell jar. Granite specimens were immersed in the water. Then, the bell jar was evacuated to remove air from the micropores of the specimens. The specimens were kept for 24 hours immersed in the distilled water in the bell jar under reduced pressure.

Experimental apparatus is shown in Fig.2. It consisted of an injection unit, a reaction unit, and a storage unit. For the reaction unit, a narrow flow channel (20 mm length, 4 mm width, and 160 μm depth) was formed from a fluoroplastic spacer (160 μm thick) with a slit (20 mm long, 4 mm wide). Two fluoroplastic base plates sandwiched the spacer and granite specimen, then everything was held together by applying pressure to downward from the top base plate and upward from the bottom base plate. A photograph of the spacer is shown in Fig.3. The roughness of the granite specimen and the bottom base plate surfaces was overcome by elastic deformation of the fluoroplastic spacer, so no leakage of solution occurred. The bottom base plate had inlet and outlet ports (0.5 mm inner diameter), for injecting or draining out radionuclide or extraction solutions, and fluoroplastic tubing was attached to each port. A blank experimental run in which the granite specimen was replaced with a fluoroplastic plate was carried out to verify the surfaces of the fluoroplastic spacer and base plates were non-reactive, then the actual experiments were done using the following procedures.

Oxide	Content (wt%)
SiO_2	69.2
Al_2O_3	15.9
K_2O	4.30
CaO	2.97
Na_2O	2.90
Fe_2O_3	2.54
P_2O_5	0.60
MgO	0.48
TiO_2	0.29
MnO	0.05
Total	99.24

Table 1. Granite chemical composition

Oxide	Content (wt%)
Quartz	37.9
Plagioclase feldspar	33.0
Potassium feldspar	18.8
Biotite	9.0
Chlorite	1.0
Prehnite	0.2
Carbonate mineral	0.1
Total	100.0

Table 2. Granite mineral composition

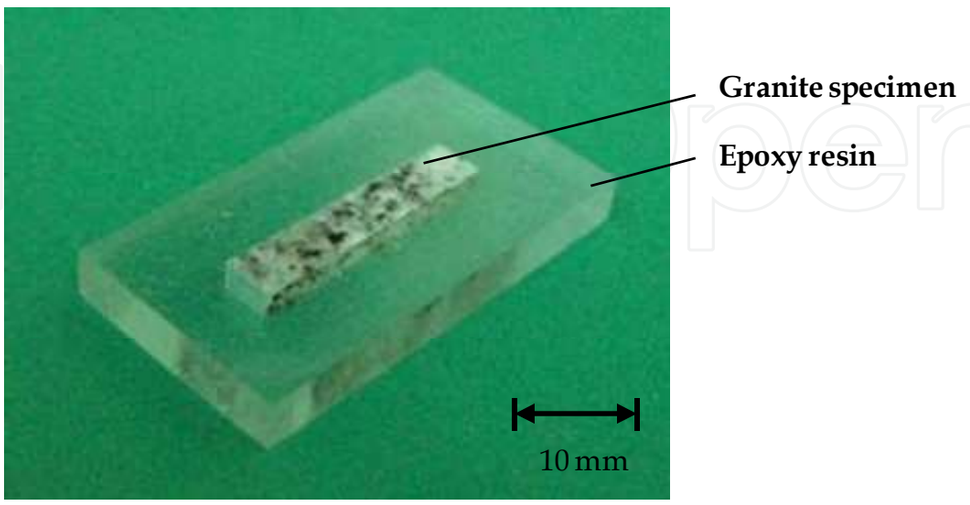

Fig. 1. Photograph of a granite specimen showing side edge surfaces coated with an epoxy resin

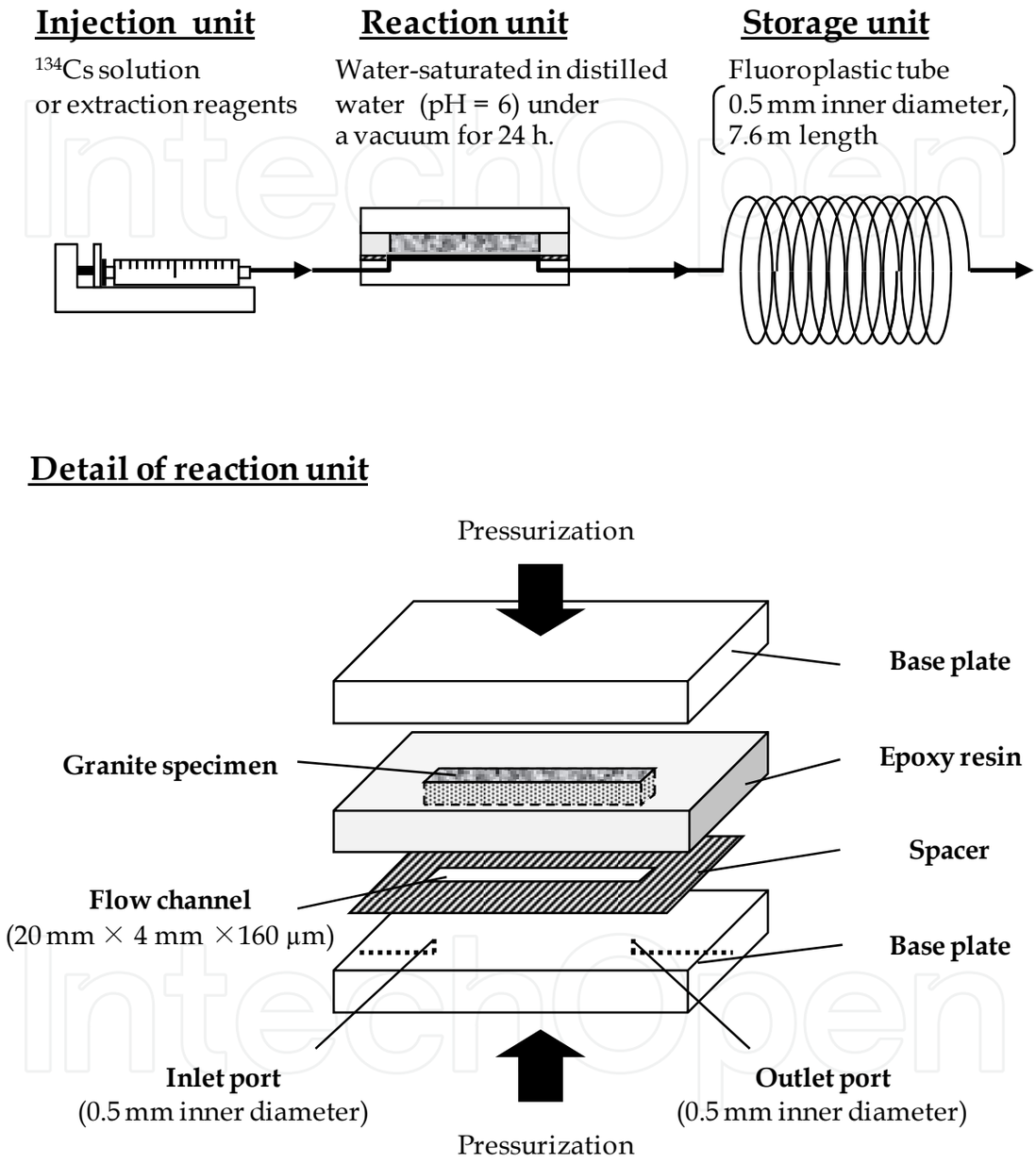

Fig. 2. Experimental apparatus for adsorption and sequential extraction experiments

In an experimental run, Cs solution labeled with ^{134}Cs (specific activity adjusted to 9.8×10^8 Bq/m^3) was injected into the flow channel at constant flow velocity (2.6×10^{-5} m/s). The flow velocity was maintained for 24 hours by using an injection pump in all experiments. Average residence time in the flow channel was 12.8 minutes. To avoid

evaporation of effluent solution during fractionation, effluent solution was stored in a storage unit (0.5 mm inner diameter, 7.6 m length). After an adsorption experimental run, the stored solution was flushed out with a high flow velocity (1.3×10^{-3} m/s), and collected in a small vial. Collection quantity was obtained precisely by weighing the vials before and after runs. The concentrations of ^{134}Cs in the effluent of the flow channel were determined with a germanium (Ge) semiconductor detector. The error of concentration measurement was less than 5%. The experimental apparatus, excluding the radioactivity detectors, was assembled in a glove box filled with air to keep dust particles off and all experimental runs were done at 25 ± 2 ˚C. After these procedures were carried out, extraction reagents were injected (Table 3) into the flow channel in sequence under the same operating conditions for the sequential extraction experiments. A series of experimental runs was carried out by changing the Cs concentration (1.0×10^{-3} - 1.0×10^{0} mol/m^3).

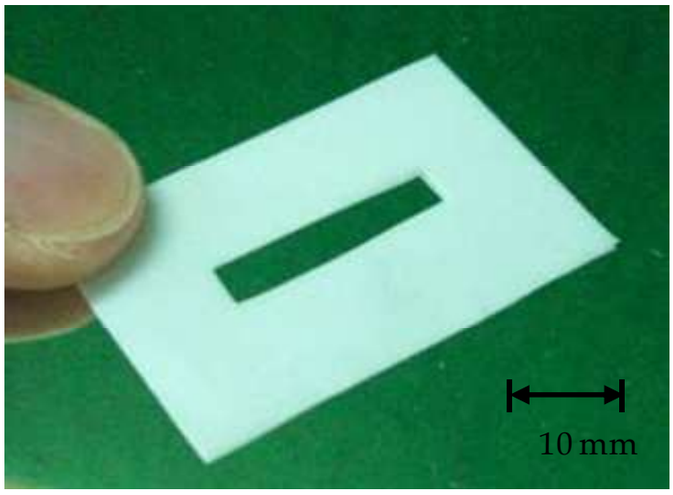

Fig. 3. Photograph of a fluoroplastic thin spacer (160 μm thick) with the slit which forms the flow channel on the granite plate

Extractant	Composition (mol/m^3)	pH
HCl	1.0×10^{-2}	5
$CaCl_2$	5.0×10^{2}	5
KCl	5.0×10^{2}	5

Table 3. Extraction reagents

2.3 Batch sorption experiment

We estimated Cs adsorption amount on granite by BTCs. In order to verify this estimation, we evaluated the retardation coefficient by analyzing BTCs, and compared it with the value calculated using the distribution coefficient (*Kd*) obtained by a batch sorption experiment. The experimental procedures for the batch sorption experiment were as follows. A granite specimen was crushed and sieved to obtain particle sizes in the range of 0.125 - 0.25 mm.

The sieved particles were rinsed with distilled water to remove the fine powder fragments. Specific surface area was measured by the BET method, and the mean value was 1.0×10^{-2} m^2/kg. Then three grams of the sieved particles was saturated with distilled water (3.0×10^{-5} m^3, adjusted to pH = 6) spiked with a radionuclide solution of ^{134}Cs (specific activity 4.9×10^7 Bq/m^3); the saturation was done under a vacuum for 24 hours to fill the granite particle pores. The initial Cs^+ solution concentrations ranged from 1.0×10^{-4} mol/m^3 to 1.0×10^2 mol/m^3. The particle-containing solutions were continuously stirred for seven days. Then the solid particles were removed by filtration through a membrane filter (pore size 0.45 μm) and the ^{134}Cs concentration was measured with the Ge semiconductor detector. The *Kd* value was calculated by the conventional procedure as follows (Holland and Lee, 1992):

$$Kd = \frac{C_{in} - C_{eq}}{C_{eq}} \cdot \frac{v}{w} \tag{1}$$

where C_{in} is initial radionuclide concentration (mol/m^3), C_{eq} is equilibrium radionuclide concentration (mol/m^3), v is solution volume (m^3) and w is rock (granite) weight (kg).

3. Analysis

We obtained the retardation coefficient by parameter identification method for BTCs using an advection-diffusion equation. The analysis object was a vertical section through the granite specimen and the flow channel as shown in Fig.4. In the calculation, the flow channel was not deep (160μm); thus we could apply a one-dimensional advection-dispersion equation. On the other hand, the permeability of granite was much small thus a two-dimensional diffusion equation was modeled. The test time was several days at the longest; therefore the radioactive decay of ^{134}Cs (half life 2.07 years) could be neglected.

The governing equations were thus formulated as follows:

For the flow channel

$$R_f \frac{\partial C_f}{\partial t} = -V \frac{\partial C_f}{\partial x} + D_L \frac{\partial^2 C_f}{\partial x^2} + \frac{D_e}{b} \frac{\partial C_m}{\partial z}\bigg|_{z=0} \tag{2}$$

$$(t > 0, \quad 0 < x < L)$$

For the granite matrix region

$$R_m \frac{\partial C_m}{\partial t} = \frac{D_e}{\varepsilon} \frac{\partial^2 C_m}{\partial x^2} + \frac{D_e}{\varepsilon} \frac{\partial^2 C_m}{\partial z^2} \tag{3}$$

$$(t > 0, \quad 0 < x < L, \quad 0 < z < d)$$

where, b is depth of the flow channel (m), $C_f(x,t)$ is radionuclide concentration in the flow channel (mol/m^3), $C_m(x,z,t)$ is radionuclide concentration in the porous granite (mol/m^3), d

is thickness of granite specimen (m), D_e is effective diffusion coefficient (m²/s), D_L is longitudinal dispersion coefficient for the flow channel (m²/s), ε is porosity of granite (-), L is length of the flow channel (m), R_f is retardation factor of granite surface (-), R_m is retardation factor of granite matrix (-), t is elapsed times (s), V is flow velocity in the flow channel (m/s), x is distance along the flow channel (m) and z is vertical distance from the flow channel (m).

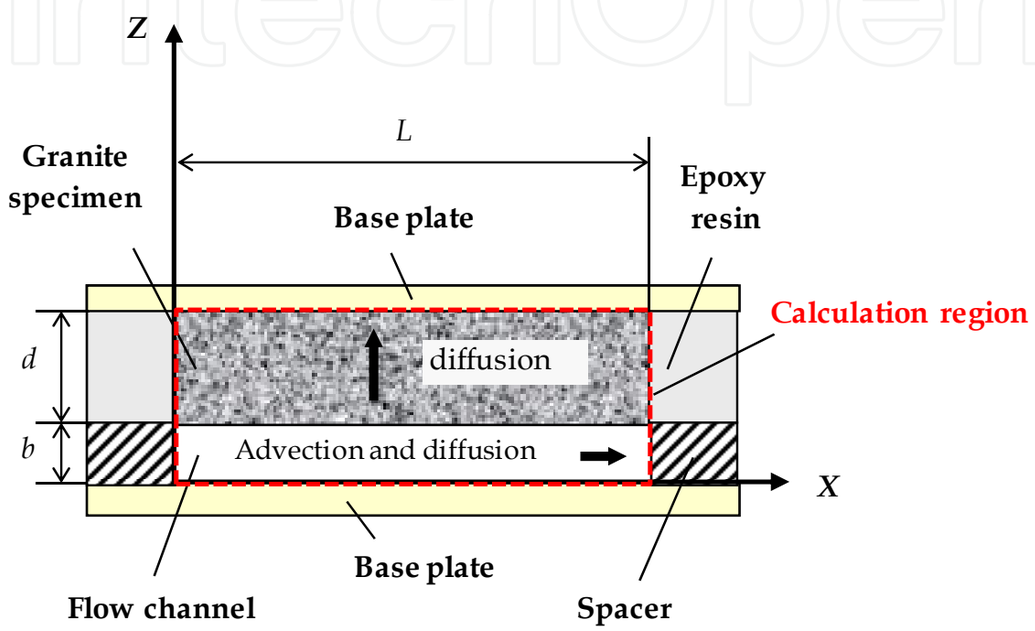

Fig. 4. Analysis object; vertical section showing the granite plate and flow channel

The boundary conditions around the flow channel were as shown in Eqs. (4) and (5):

$$VC_f - D_L \left.\frac{\partial C_f}{\partial x}\right|_{x=0} = \frac{F}{A}, \quad (t > 0) \tag{4}$$

$$C_m(x,0,t) = C_f(x,t), \quad (0 < x < L, \quad t > 0) \tag{5}$$

where, F is the inlet flux of radionuclide (mol/s) and A is cross sectional area of the flow channel (m²).

Other boundary conditions around the granite specimen were as shown in Eqs. (6) – (8):

$$\frac{\partial C_m(x,d,t)}{\partial z} = 0, \quad (0 < x < L, \ t > 0) \tag{6}$$

$$\frac{\partial C_m(0,z,t)}{\partial x} = 0, \quad (0 < z < d, \ t > 0) \tag{7}$$

Symbol	Parameter	Value
A	Cross sectional area of the flow channel	6.4×10^{-7} m²
b	Depth of the flow channel	1.6×10^{-4} m
d	Thickness of granite specimen	3.0×10^{-3} m
D_e	Effective diffusion coefficient	1.5×10^{-11} m
D_L	Longitudinal dispersion coefficient for the flow channel	0 m²/s
D_{Lst}	Longitudinal dispersion coefficient for the storage unit	3.0×10^{-5} m²/s
ε	Porosity of granite	0.73 %
L	Length of the flow channel	2.0×10^{-2} m
L_{st}	Length of the storage unit	7.6 m
t	Elapsed times	86400 s.
V	Flow velocity in the flow channel	2.6×10^{-5} m/s
V_{st}	Flow velocity in the storage unit	1.3×10^{-3} m/s

Table 4. BTCs calculation condition and parameters

$$\frac{\partial C_m(L, z, t)}{\partial x} = 0, \quad (0 < z < d, \ t > 0) \tag{8}$$

The calculation parameters are given in Table 4. The effective diffusion coefficient (D_e) was related to the diffusion coefficient in free water (D_0) and the formation factor (FF) (Skagius, et al., 1982) as given by Eq.(9):

$$D_e = \varepsilon \cdot \frac{\delta}{\tau^2} \cdot D_0 = FF \cdot D_0 \tag{9}$$

where, δ is constrictivity (-) and τ^2 is tortuosity (-). The value of FF for ^{3}H was used instead of that for ^{134}Cs because non-sorbing characteristics of ^{3}H lead to direct determination of FF as shown in Eq. (10):

$$FF = \left(\frac{D_e}{D_0} \right)_{^3H} \tag{10}$$

The values of D_e and D_0 for ^{3}H are 1.5×10^{-11} m²/s (Okuyama, et al., 2008) and 2.00×10^{-9} m²/s (Chemical Society of Japan, 2004), respectively. By substituting the values of D_0 for Cs as 2.04×10^{-9} m²/s (Chemical Society of Japan, 2004) into Eq. (9), we obtained $D_e = 1.5 \times 10^{-11}$ m²/s for Cs; we used this value for BTC analysis.

When the Cs-containing solution flowed through the flow channel and storage unit, it was dispersed in the longitudinal direction. The length of the flow channel (20 mm) was much shorter than that of the storage unit (7.6 m length), thus we neglected dispersion in the flow channel. In order to obtain longitudinal dispersion coefficient for the storage unit D_{Lst}, we calculated the value of the dispersion length a by analyzing the one-dimensional advection-dispersion equation as Eqs. (11) and (12):

$$\frac{\partial C_{st}}{\partial t} = -V_{st}\frac{\partial C_{st}}{\partial x} + D_{Lst}\frac{\partial^2 C_{st}}{\partial x^2} \tag{11}$$

$$\left(t > 0,\quad 0 < x < L_{st}\right)$$

$$D_{Lst} = D_0 + a \cdot V_{st} \tag{12}$$

where, a is dispersion length (m). $C_{st}(x, t)$, L_{st} and V_{st} are radionuclide concentration (mol/m^3), length (m) and flow velocity (m/s), in the storage unit, respectively.

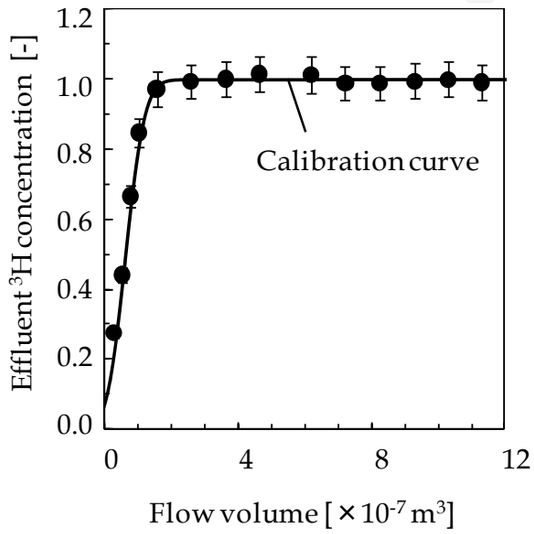

Fig. 5. Experimental BTC values of ^{3}H with the calibration curve using the results of the numerical analysis

The BTC of ^{3}H, which is a non-sorbing species, is shown in Fig. 5. In a blank experimental run, we confirmed that ^{3}H was not absorbed on the fluoroplastic tubing, thus the outlet concentration agreed with the inlet concentration (C_{st} / C_0 = 1). The transient region to the value of C_{st} / C_0 = 1 represented the effect of dispersion in the storage unit. The value of a was determined by a parameter identification method and a = 0.023 m was obtained. By substituting the values of a into Eq. (12), we obtained D_{Lst} = 3.0 ×10^{-5} m^2/s for storage unit; thus this value was used for BTC analysis. Equations (2) and (3) were solved, subject to Eqs.(4)-(8), using a finite volume scheme.

4. Results and discussion

4.1 Adsorption of ^{134}Cs

We evaluated Cs adsorption amount on granite by BTCs. BTCs was obtained by injecting the Cs solution labeled with ^{134}Cs into the flow channel at constant flow velocity. Figure 6 plots BTCs of ^{134}Cs for various inlet Cs concentrations, showing the change in normalized effluent concentration C/C_0, which is the effluent concentration C divided by the inlet

concentration C_0, as a function of elapsed time. A quasi-plateau region was observed for each curve and the breakthrough values in this region did not reach the equilibrium $C/C_0 = 1$. This is because some of the Cs may be still driven away by diffusion into the granite matrix or they were absorbed on the rock surface. From the mass balance standpoint, we assumed that the area enclosed by the lines of $C/C_0 = 1$ and the BTC represented the Cs diffusion into the granite matrix or the Cs absorbed on the granite surface.

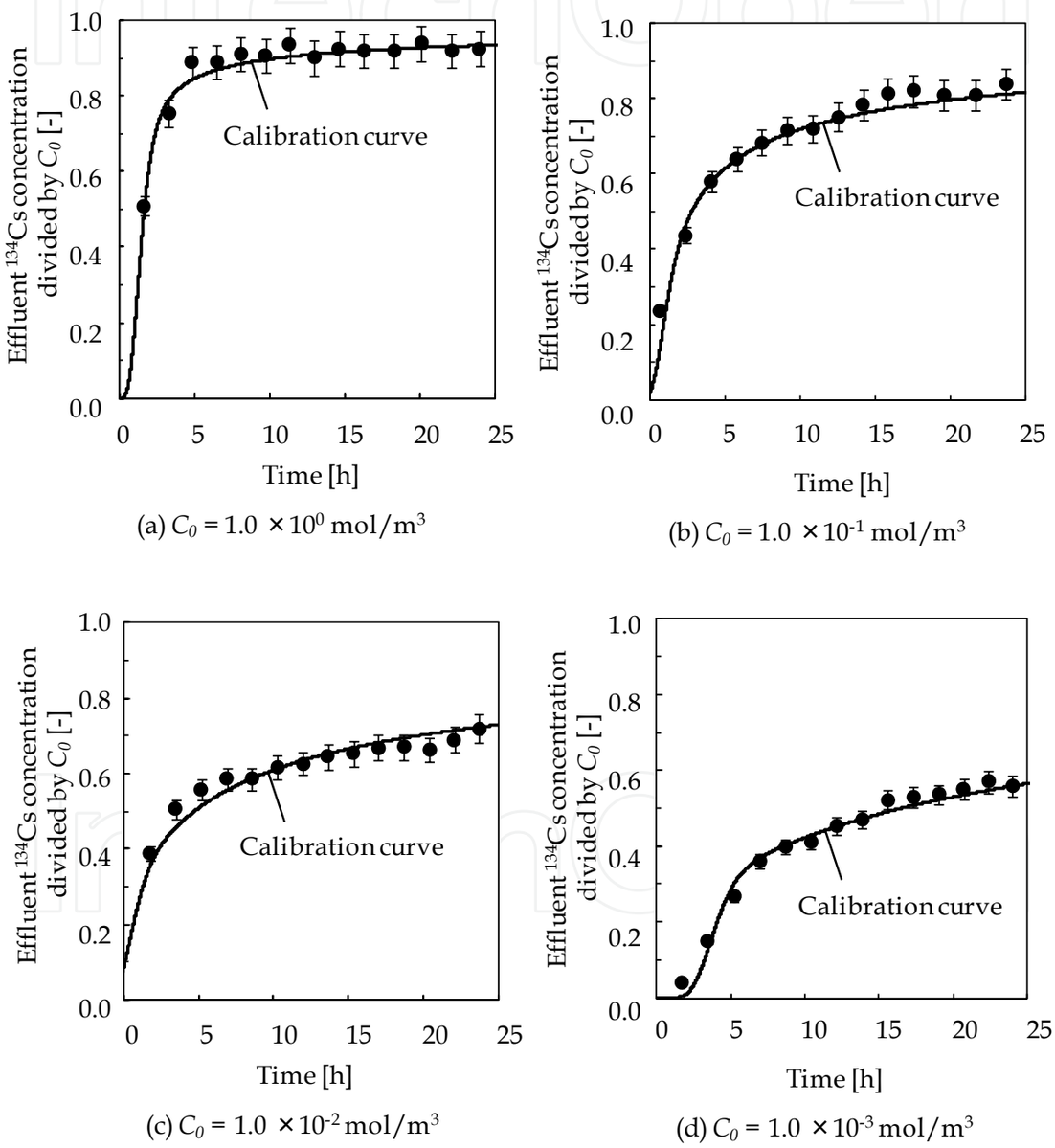

Fig. 6. Experimental BTCs of ^{134}Cs for various inlet Cs concentrations with a curve using the result of the numerical analysis

In order to verify this estimation of sorption amount, we determined the retardation coefficient by parameter identification method for BTCs using Eqs. (2), (3), and (11), and compared it with the retardation coefficient (R_m) calculated using the value of Kd obtained by a batch sorption experiment. By inserting ε, Kd, and density of granite ρ (2.98 ×10^3 kg/m^3) into Eq.(13), R_m were calculated.

$$R_m = 1 + \frac{\rho \cdot Kd}{\varepsilon} \tag{13}$$

The R_m values obtained by the two methods were almost identical, therefore the area enclosed by the lines of C/C_0 = 1 and BTC represented the Cs diffusion into the granite matrix or the Cs absorbed on the rock surface (Okuyama, et al., 2008).

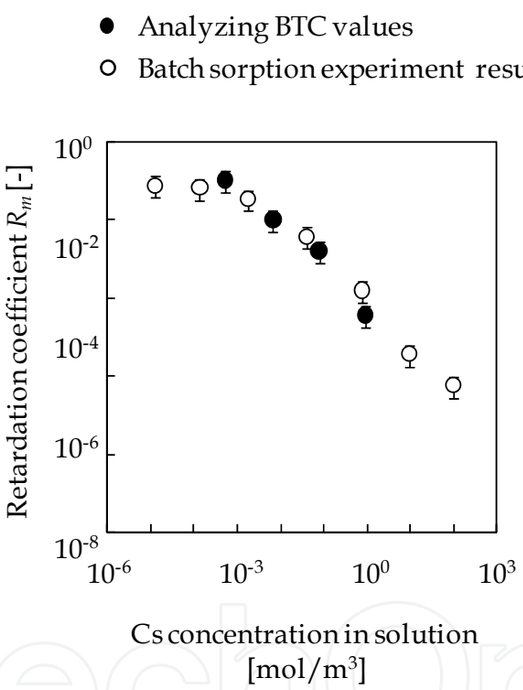

Fig. 7. Retardation coefficients obtained by analyzing BTC values and batch sorption experiment results

4.2 Desorption of ^{134}Cs

After injecting ^{134}Cs solution, extraction reagents (HCl, $CaCl_2$, and KCl solutions as shown in Table 3) were injected into the flow channel in sequence. We obtained the desorption curves and investigated the chemical speciation of Cs in granite, in particular the ratio of the density of reversible and irreversible adsorption sites depends on Cs concentration in solution. Desorption curves are shown in Fig. 8 as the change in normalized desorbed Cs divided by the total adsorption amount. For each curve, desorption amount of Cs was significantly decreased to 1 % or lower when elapsed time was 24, 48, and 72 hours, so Cs

was adequately desorbed by each reagent. Desorption amount of Cs changed drastically between the reagents, thus it was conceivable that desorbed Cs for each reagent indicated the presence of multiple adsorption sites.

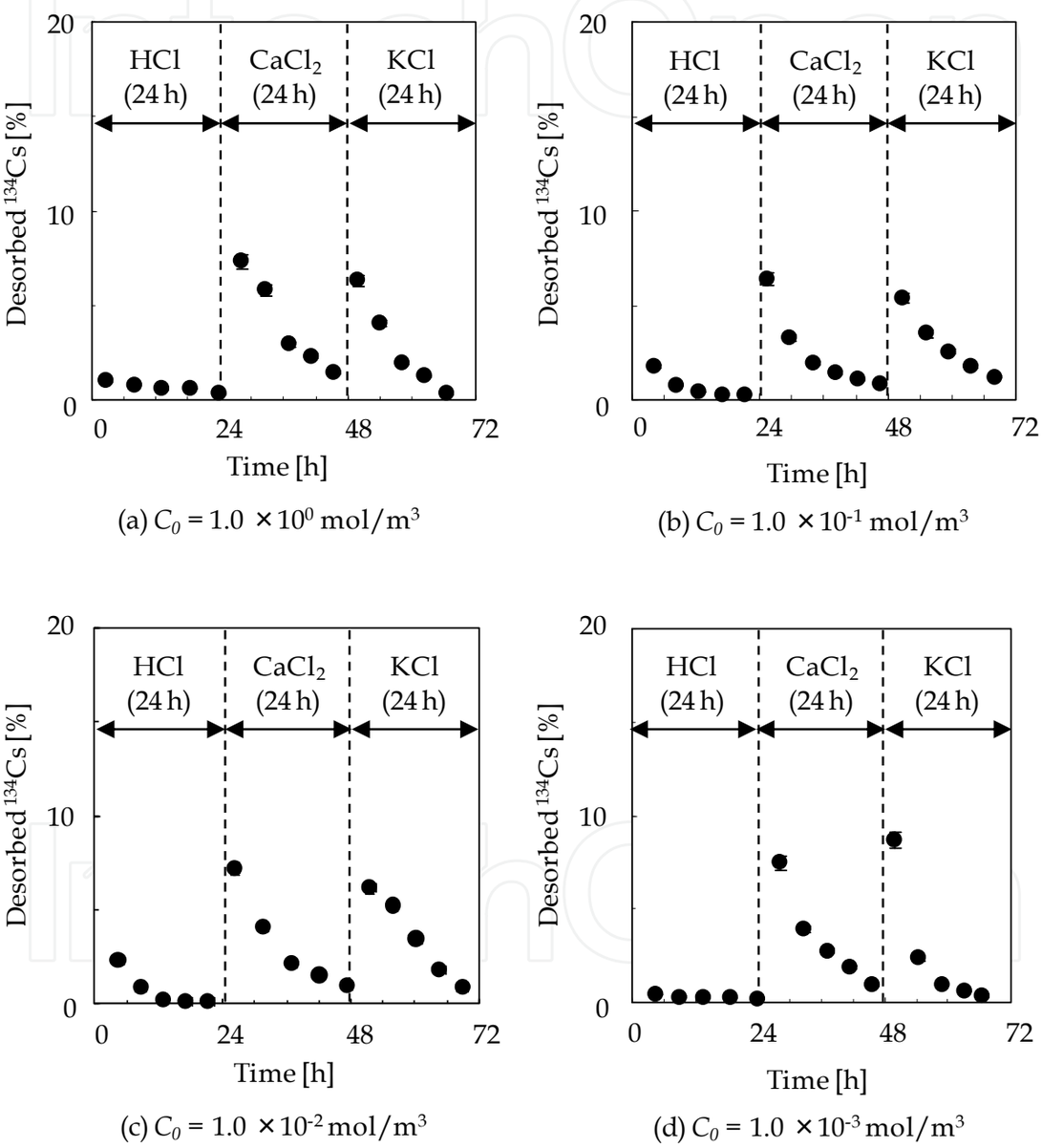

(a) $C_0 = 1.0 \times 10^{0}$ mol/m^3 (b) $C_0 = 1.0 \times 10^{-1}$ mol/m^3

(c) $C_0 = 1.0 \times 10^{-2}$ mol/m^3 (d) $C_0 = 1.0 \times 10^{-3}$ mol/m^3

Fig. 8. Experimental desorption curves of ^{134}Cs for various inlet Cs concentrations

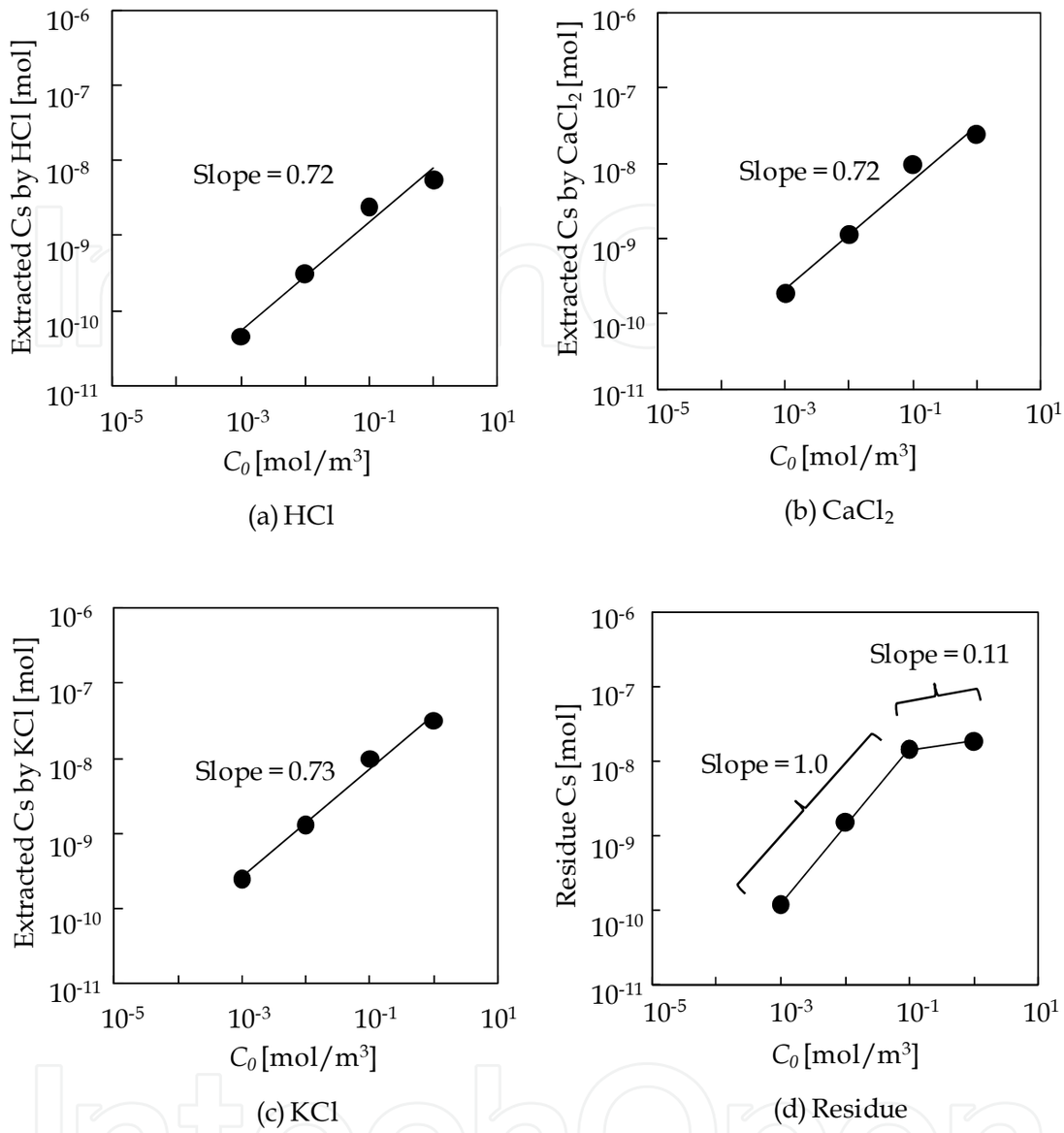

Fig. 9. Desorbed amounts of Cs at various quasi-plateau Cs concentration of BTCs

Desorption amount of Cs at various quasi-plateau Cs concentration of BTCs is summarized in Fig. 9. The fractions extracted with HCl, KCl and $CaCl_2$ gave straight lines and the slopes were about 0.7, which could be described by a Freundlich isotherm. On the other hand, the residue fraction was directly proportional to the Cs concentration at low Cs concentration (lower than 1×10^{-1} mol/m^3), and showed signs of leveling off at 1×10^{0} mol/m^3; thus Cs adsorption on granite surface may become saturated at Cs concentration of 1×10^{0} mol/m^3.

The chemical speciation of Cs desorbed by each regent was described as follows. Biotite has two types of adsorption sites; variable-charge sites, and permanent-charge sites. The charge of variable-charge sites changes with changing pH, thus the fraction of Cs extracted with HCl indicates adsorption amount on variable-charge sites. On the other hand, it has been

reported that Cs is strongly absorbed on biotite grains; in particular it is distributed onto the interlayers of these grains[2], which is permanent-charge sites. The hydrated ionic radius of K^+ (0.13 nm) (Ohtaki, 1990) are almost identical to that of Cs^+ (0.12 nm) (Ohtaki, 1990), thus Cs^+ which has been taken into the interlayers induces interlayer spacing that is large enough to permit diffusion of K^+; thus K^+ would displace adsorbed Cs on the biotite interlayer permanent-charge sites. The hydrated ionic radius of Ca^{2+} (0.31 nm) (Ohtaki, 1990) is much larger than that of Cs^+ and Ca^{2+} diffusion into the interlayers is restricted (Cornell, 1993); thus Ca^{2+} would displace adsorbed Cs on the edge of the biotite interlayer or at other mineral sites such as feldspar (Brown, et al., 1984). From the above, although the chemical speciation of Cs desorbed for the three regents was different, the adsorption mechanism of Cs for each was an ion-exchange reaction. The adsorption mechanism of the residue fraction might be fixed in biotite[2]. In this study, we defined that as irreversible adsorption.

The fraction of Cs desorbed by the three reagents is shown in Fig. 10. The sum of fractions extracted with HCl, $CaCl_2$ and KCl, which indicated reversible adsorption, was 60 - 80 %. Irreversible adsorption was relatively large at high Cs concentration. However, Cs adsorption was saturated at 1 $\times 10^0$ mol/m^3, and the fraction of irreversible adsorption decreased.

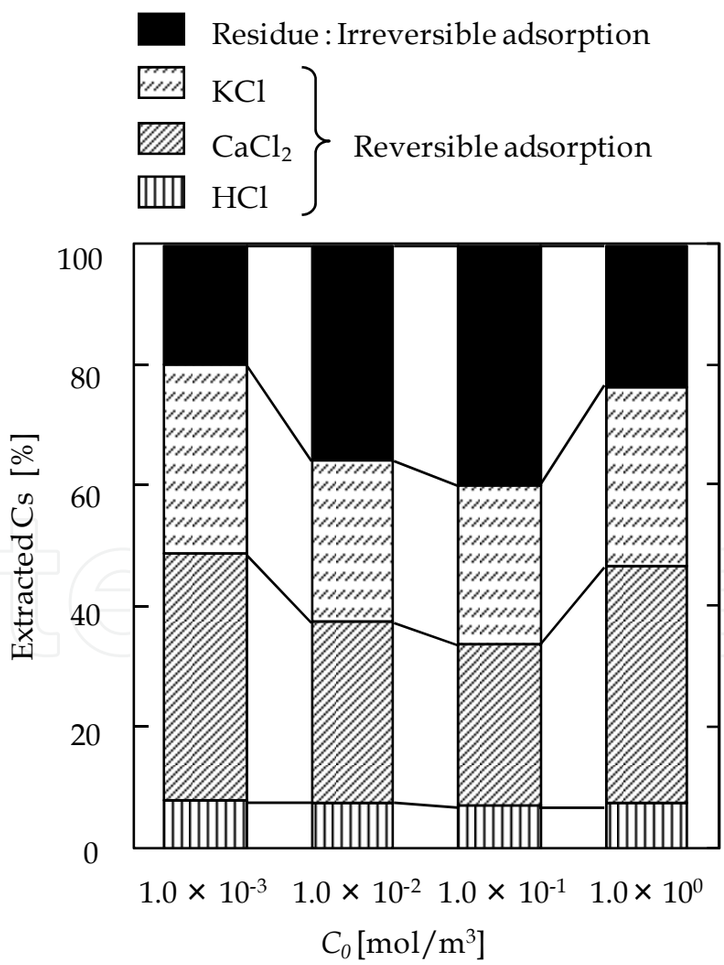

Fig. 10. Fraction of Cs desorbed by three extraction reagents (HCl, $CaCl_2$, KCl)

When the irreversible sites are saturated, the Cs will no longer be retarded by them. Thus, it is concluded that the ratio of the density of reversible and irreversible adsorption sites must be thoroughly considered to demonstrate the safety of HLW deep underground disposal option.

5. Conclusion

We carried out adsorption and sequential extraction experiments using three chemical reagents (HCl, $CaCl_2$, and KCl solutions) for various inlet Cs concentrations to investigate the chemical speciation of Cs in granite. In particular, we focused on the dependence of adsorption amount on reversible and irreversible sites on Cs concentration. The sum of fractions extracted with HCl, $CaCl_2$ and KCl, which indicated reversible adsorption, was 60 - 80 %. Irreversible adsorption was relatively large at high Cs concentration. However, Cs adsorption became saturated, and the fraction of irreversible adsorption decreased. Cs adsorption on granite surface was saturated at Cs concentration of 1×10^0 mol/m^3. In the early stage of radionuclide leakage, Cs will be retarded by the presence of reversible and irreversible adsorption sites. However, when the irreversible sites were saturated, Cs will not be retarded by them. Thus, the sorption reversibility must be thoroughly considered to demonstrate the behavior of Cs in granite, in particular for high Cs concentration.

6. References

Brown, D. L., Haines, R. I., Owen, D. G., Stanchell, F. W. & Watson, D. G. (1984). Surface studies of the interaction of cesium with feldspars. *American chemical society*, 246, pp. 217-227

Cornell, R. M. (1993). Adsorption of cesium on minerals: A review. *J. Radioanalytical and Nuclear Chemistry*, 171, 2, pp. 483-500

Francis, C. W. & Brinkley F. S. (1976). Preferential adsorption of ^{137}Cs to micaceous minerals in contaminated freshwater sediment. *Nature*, 260, pp. 511-513

Fukui, M. (2004). Affinity of trace elements to sandy soil and factors affecting on the migration through media. *KURRI KR*, 99, pp. 21-26

Holland, T. R. & Lee, D. J. (1992). Radionuclide getters in cement. *Cement and Concrete Research*, 22, pp. 247-258

Chemical Society of Japan. (Ed.). (2004). *Kagaku Binran, Basic 5th ed.,* Maruzen Company, Tokyo, pp. 64-65

Ohe, T. (1984). Ion exchange adsorption of radioactive cesium, cobalt, manganese, and strontium to granitoid rocks in the presence of competing cations. *J. Nucl. Sci. Technol.*, 67, 1, pp. 92-101

Ohtaki, H. (1990). Hydration of Ions. *Kyoritsu Shuppan,* Tokyo, pp. 55

Okuyama, K., Sasahira, A., Noshita, K., & Ohe, T. (2008). A method for determining both diffusion and sorption coefficients of rock medium within a few days by adopting a micro-reactor technique. *Applied Geochemistry*, 23, pp. 2130-2136

Peech, M. (1965). Exchange acidity: Barium chloride-triethanolamine method. *Methods of soil analysis*, *Part 2*, American Society of Agronomy, Madison, Wisconsin, pp. 910–911

Skagius, K. & Neretnieks, I. (1982). Diffusion in crystalline rock. *Nucl. Waste Manage.*, 5, pp. 509–518

Skagius, K. & Neretnieks, I. (1986). Porosities and diffusivities of some non-sorbing species in crystalline rocks. *Water Resour. Res.*, 22, pp. 389-398

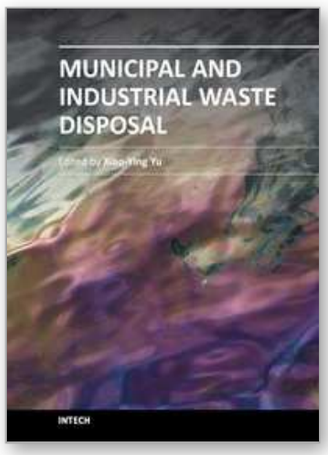

Municipal and Industrial Waste Disposal

Edited by Dr. Xiao-Ying Yu

ISBN 978-953-51-0501-5
Hard cover, 242 pages
Publisher InTech
Published online 11, April, 2012
Published in print edition April, 2012

This book reports research findings on several interesting topics in waste disposal including geophysical methods in site studies, municipal solid waste disposal site investigation, integrated study of contamination flow path at a waste disposal site, nuclear waste disposal, case studies of disposal of municipal wastes in different environments and locations, and emissions related to waste disposal.

How to reference

In order to correctly reference this scholarly work, feel free to copy and paste the following:

Keita Okuyama and Kenji Noshita (2012). Clarification of Adsorption Reversibility on Granite that Depends on Cesium Concentration, Municipal and Industrial Waste Disposal, Dr. Xiao-Ying Yu (Ed.), ISBN: 978-953-51-0501-5, InTech, Available from: http://www.intechopen.com/books/municipal-and-industrial-waste-disposal/clarification-of-adsorption-reversibility-on-granite-that-depends-on-cesium-concentration

INTECH
open science | open minds

InTech Europe
University Campus STeP Ri
Slavka Krautzeka 83/A
51000 Rijeka, Croatia
Phone: +385 (51) 770 447
Fax: +385 (51) 686 166
www.intechopen.com

InTech China
Unit 405, Office Block, Hotel Equatorial Shanghai
No.65, Yan An Road (West), Shanghai, 200040, China
中国上海市延安西路65号上海国际贵都大饭店办公楼405单元
Phone: +86-21-62489820
Fax: +86-21-62489821

IntechOpen